EIGHTH EUROPEAN ROTORCRAFT FORUM

Paper No. 7.2

FURTHER APPLICATION AND DEVELOPMENT OF STRAIN PATTERN ANALYSIS

A. R. Walker

Royal Aircraft Establishment,
Farnborough, England

SUMMARY

Further application of Strain Pattern Analysis (SPA) to the derivation of vibration mode shapes of a rotating blade is described. A model blade representative of a typical semi-rigid rotor system is used as the test structure. Modes are derived for both non-rotating and rotating conditions with the blade shielded from aerodynamic loading in the latter case. The experimentally derived modes are compared with corresponding calculated modes. A discussion of a theoretical exercise undertaken to investigate the distribution of strain measurement stations required for successful application of SPA is also included.

31 August - 3 September, 1982
Aix-en-Provence, France

CONTENTS

1 INTRODUCTION

In recent years, new helicopter rotor blade designs have appeared in which the mass and stiffness distributions are manipulated to give required couplings between flap, lag and torsion components of motion. Such couplings influence almost every aspect of rotor dynamic behaviour, and analytical investigations of their effects rely heavily on an accurate mathematical model of the modes of vibration of the blades. Calculation methods giving mode shapes and frequencies are readily available but some experimental verification of them is necessary. The technique of Strain Pattern Analysis (SPA) has been developed at RAE[1-3] to derive the mode shapes of a rotating blade from the responses of strain gauges located on the blade.

The application of SPA is, in principle, quite simple. In Ref 1, Gaukroger and Hassal proposed that if a certain pattern of strain gauge responses were measured for a rotating blade, and if the same pattern of responses could be reproduced with the blade non-rotating, then the displacements in the two conditions would be the same. Further, if the strain gauge responses of a mode of the rotating blade could be represented by a linear summation of the strain gauge responses of several modes of the non-rotating blade, then the unknown rotating mode shape would be given by the same linear summation of the known displacements of the non-rotating blade.

The SPA technique has been applied to a model helicopter rotor blade which was representative of a semi-rigid rotor system. Modes for both non-rotating and rotating conditions have been derived, with the blade shielded from the bulk of aerodynamic loads in the latter case. The experimentally derived modes were compared with corresponding blade modes as calculated by a theoretical method. Some discrepancies occurred between theory and experiment but the general level of agreement was good, particularly in the lower order modes.

The rotor blade model used in the experiments had a root flexural member in which the flap stiffness was low relative to that of the remainder of the blade. The experimental evidence suggested that an insufficient number of strain gauges in this area could lead to inaccurate derivation of higher order mode shapes. Hence a theoretical study was undertaken to investigate the distribution of strain gauges required for successful application of SPA to semi-rigid rotor blade systems. Some of the results are presented in the paper and they indicate that strain gauges must be concentrated in areas where there is a high rate of change of strain with respect to the blade spanwise coordinate, *eg* in areas of changing flexibility.

The original concept of SPA was to develop a method which would verify theoretical mode predictions. This objective has been largely achieved and it now remains to develop the technique to its full potential. Experiments have already begun to extend SPA to both wind tunnel and full-scale flight test applications with the aim of deriving instantaneous displacements of the rotating blade.

2 THEORETICAL BACKGROUND

The theoretical background of the SPA technique is well documented[1-3] and therefore only a brief summary will be given. Two conditions must be met if the application of the technique is to be valid; firstly, that there is a unique relationship between the strain responses and corresponding displacement patterns within a mode and, secondly, that sufficient non-rotating

modes must be defined such that a linear combination of them will provide a good approximation to the rotating mode.

Let us assume that the blade is instrumented with r strain gauges and n displacement transducers and let p sets of non-rotating strain and displacement patterns be measured. These patterns are known as 'calibration' modes. If for some rotating test condition for which the displacement pattern is unknown we measure a set of r strain gauge responses denoted by x, then for a least-squares error fit it has been shown[1-3] that the proportion, α, of each calibration mode present in the unknown test mode is given by

$$\alpha = (S^T S)^{-1} S^T x \qquad (\text{if } r \geqslant p) \ ,$$

where S is the $r \times p$ matrix of the calibration strain patterns. Assuming that the unknown displacement pattern, δ, is given by the same linear sum of the calibration displacement patterns, then

$$\delta = D\alpha = D(S^T S)^{-1} S^T x \ ,$$

where D is the $n \times p$ matrix of the calibration displacements corresponding to the calibration strain patterns S. Although the number of strain gauge and displacement measurement positions need neither be the same nor coincide, both must be capable of accurately representing the changing strain and displacement distributions along the blade span.

3 EXPERIMENTAL ROTOR TESTS

A detailed description of the blade model and the instrumentation used in the tests is given in Ref 4. Briefly, the model represented a typical semi-rigid rotor blade (Fig 1) possessing a flexible element in the root area which had a low stiffness compared with that of the remainder of the blade. The blade was not an exact scale model of any existing full-scale blade but the mass and stiffness distributions were chosen to give mode shapes and frequencies representative of a helicopter blade.

Strain gauges sensitive to motion in flap, lag and torsion were situated at ten equally spaced intervals along the blade from 5% to 95% blade radius. Calibration modal displacements in the three directions of motion were also measured at ten equally spaced intervals (from 10% to 100% blade radius) by non-contacting capacitance probes. Flap and lag motions were defined as displacements measured from the blade ¼-chord position; torsion motions were calculated from differential flap measurements.

Mode excitation was obtained from an electromagnetic vibrator located at the blade root and attached to the blade by an offset crank (Fig 2). The excitation was controlled by RAE MAMA equipment[5] which automatically maintained a resonance condition by ensuring a quadrature phase relationship between the force input and the response of a continuously monitored reference strain gauge sensitive to motion in the main component of the mode under investigation. It should be noted that, with single-point excitation, only an approximation to undamped modes can be obtained.

The strain patterns and corresponding displacements were recorded for the first ten modes of the non-rotating blade. These modes were the 'calibration' modes of the blade. The capacitance probes were then removed from the structure and the strain responses of the first eight modes of the blade were recorded for a selection of rotational speeds including a

non-rotating case. These modes are subsequently referred to as the 'test' modes of the blade. As one of the main aims of SPA development was to measure blade modes for comparison with theory, the rotating blade was shielded from the bulk of aerodynamic loads by enclosing it within a segment of a hollow disc. The disc was attached to the hub and rotated with the blade. By this method, all test modes of the blade were in 'still air' conditions for both non-rotating and rotating cases. The shielding disc is shown in Fig 3 and the blade housed in its segment, with the access cover removed, in Fig 4.

Before the results are considered the effect of phase differences along the blade should be discussed. Phase shifts in the strain responses along the blade were measured in order that both in-phase and quadrature components of each mode could be investigated. The phase reference chosen was the response of the continuously monitored strain gauge used to control the excitation. In the calibration modes, only small phase shifts were detected and it was assumed that all responses of the calibration modes were everywhere in-phase. This assumption simplified the subsequent analysis of the test modes in that it enabled the in-phase and quadrature responses to be processed separately. In general, quadrature components of motion in the test modes were small compared with the in-phase components.

4 COMPARISON WITH CALCULATED MODES

Modal displacements and frequencies of the blade model were calculated from known distributions of its mass, stiffness and inertia by a theoretical method developed by Westland Helicopters Ltd (WHL)[6]. The modes obtained by calculation did not include the effects of aerodynamic loading, structural damping or Coriolis forces. Therefore the mode shapes were the undamped modes of the blade which in the rotating condition were modified by centrifugal loads only. The result of these simplifications was that blade responses in any mode were in-phase (or anti-phase) and so phase shifts along the blade did not arise. Consequently the calculated mode shapes could be compared with the in-phase components of the experimentally derived modes.

Although mode shapes and frequencies were calculated for each test mode at all the rotational speeds adopted in the experiment[7], only those at a rotor speed of 8 rev/s are presented (see Figs 5 to 12). It should be noted that, for both calculated and experimentally derived modes, the mode shapes have been non-dimensionalised by dividing each modal component by the largest component of motion within the mode, which itself then became unity. The torsion angular component was multiplied by the blade chord before such 'normalisation' took place.

Consider initially the primary components of the modes. It can be seen that, apart from two exceptions, the agreement between the calculated mode shapes and those derived by SPA is good. The exceptions are test modes 4 and 5 (Figs 8 and 9) for which the calculations give two distinct modes, *ie* fundamental torsion at a frequency of 86.9 Hz and second overtone flap at a frequency of 90.4 Hz. However, due to the limitations of single-point excitation it was not possible to isolate these two modes in the experiment. The experimental modes shown were obtained using a torsion strain gauge as a reference for the control of the excitation in the case of test mode 4 (Fig 8), whilst test mode 5 (Fig 9) used a flap strain gauge. The measured frequencies were 91.6 Hz and 92.2 Hz respectively and the mode shapes are virtually identical. Although not shown in Fig 9, there was a significant phase shift along the blade for test mode 5 producing a large quadrature

torsion component of motion. It can be seen that the experimental determination of these two modes (if indeed two modes exist) was far from ideal.

The comparison between secondary components of the modes is not as good. The worst case is test mode 6 (Fig 10), the first overtone lag mode. Here the experimentally derived flap component appears to have a greater tip displacement than the derived primary lag component. The reason for this is thought to be an insufficient number of strain gauges on the root flexible element. This can lead to inaccurate mode derivation because the rapid changes in strain over the small spanwise segment of the root flexure are not represented in the strain gauge responses. This is discussed more fully in section 5.

There are, of course, many reasons for discrepancies between the calculated and experimentally derived mode shapes. There are inevitable errors in the data used in the calculation of the mode shapes due primarily to inaccuracies in measurements of the mass, stiffness distributions, etc of the blade system. Any small discrepancies that do occur in these distributions can significantly affect the secondary components of the calculated mode shapes. Furthermore, the effect of structural damping is not included in the theoretical method and also the assumption of root rigidity in the calculation implies an infinite inertia in the axial or lag sense; in the experiment, only an approximation to fixed-root conditions was achieved. Although small, some error certainly existed in the measurement of the calibration displacement patterns and to a lesser extent in the measurement of the strain responses. Nevertheless, the general level of agreement between calculated and derived mode shapes is good, particularly in the lower order modes. This applies to both non-rotating and rotating conditions of the blade. Although the comparisons are not exhaustive they largely achieve the original objective of SPA - to develop an experimental method which can verify theoretical mode predictions.

5 STRAIN GAUGE DISTRIBUTION

As stated previously, it was noted that some errors occurred when SPA was used to derive the higher order mode shapes. The experimental evidence suggested that an insufficient number of strain gauges in the root area of high flexibility could cause significant inaccuracies when deriving the higher order mode shapes of the rotating blade. Therefore it was decided that a theoretical exercise should be undertaken[8] to determine the distribution of strain gauges required for the accurate application of SPA.

Four distributions of assumed strain measurement stations were adopted in the investigation, the differences being the number and positioning of the stations along the blade. These distributions are subsequently referred to as A, B, C and D, and are shown in Fig 13. Distribution A consisted of the same strain measurement stations as used in the experiment, *ie* ten equally spaced stations, whereas distribution B had twenty equally spaced stations from 5% blade radius to 100% blade radius. Distribution C had the same ten stations as distribution A plus an extra six concentrated on the flexible element in the root area. Finally distribution D had the same twenty stations as distribution B plus an extra four also concentrated on the root flexible element. The number of displacement measurement stations was kept constant in all four cases, *ie* ten equally spaced stations from 10% blade radius to 100% blade radius.

Modes were calculated for the blade using the WHL theoretical method[6] described previously. Strain and displacement responses were calculated

for each mode in each of the three degrees of freedom, namely flap, lag and torsion. The calibration modes adopted were the non-rotating modes of the blade. The calculated strain responses for modes of the rotating blade were used to derive the corresponding blade mode shapes which were then compared with those calculated by the theoretical method of mode prediction.

As an example of the results, consider two modes of the blade rotating at a speed of 8 rev/s. In the first mode, the second overtone flap (Fig 14), the primary flap component is not derived accurately unless the strain measurement stations are concentrated in the root area of changing flexibility (distributions C and D). Note that the other components of the mode are unaffected. Consider now the strain patterns associated with this mode (Fig 15). It can be seen clearly that only distributions C and D represent the rapidly changing strain variation in the blade root area. This observation is also true for the second mode, the third overtone flap (Fig 16), where again the primary flap component is only derived accurately when the strain measurement stations are concentrated in the areas of rapidly changing strain (Fig 17). These observations also apply to other modes of the rotating blade. If the proportions of the calibration modes present within each derived mode are examined (see Tables 1 and 2), it is found that the amount of the fundamental flap calibration mode is substantially reduced when the strain measurement stations are concentrated in the root areas of changing flexibility (distributions C and D). Higher order calibration mode proportions alter insignificantly. The strain patterns of the fundamental flap calibration mode are shown in Fig 18. It can be seen that neither distribution A nor distribution B accurately represents the strain distribution of the primary mode component, whereas the high rate of change of strain in the root area is represented in distributions C and D. Note that distribution C adequately defines the strain variation in the outer regions of the blade, and that the extra strain measurement stations included in this area in distribution D are therefore superfluous.

For the blade model considered, the most rapid strain variation with respect to the spanwise coordinates occurs close to the blade root on the flexible element, especially in the flap component of motion. When the maximum number of strain measurement stations is used to define the root strains (distributions C and D), the proportion of the fundamental flap calibration mode is relatively small and an accurate mode shape is derived. However, this proportion is greatly increased when the minimum number of strain measurement stations is used (distributions A and B), and consequently the agreement between calculated and derived mode shapes is poor.

In conclusion, it can be stated that for successful application of SPA to a semi-rigid rotor blade, the strain measurement stations must be concentrated in the areas where a high rate of change of strain with respect to the span occurs, so that an adequate representation of the variation appears in the strain patterns. In practice, this means concentrating strain gauges in the areas of changing flexibility.

6 CONCLUDING REMARKS

Further application and development of strain pattern analysis (SPA) with reference to a semi-rigid rotor system has been described. Derived mode shapes, which include displacements or rotations in the flap, lag and torsion components of motion, are presented for the rotating blade. A comparison is included with corresponding calculated mode shapes. The level of

agreement is good and it can be stated with some confidence that a method has been developed to verify theoretically predicted mode shapes. A description is also included of a theoretical exercise undertaken to investigate the required distribution of strain gauges for successful application of SPA. The results indicate that strain gauges must be concentrated in the areas of changing flexibility where there is a high rate of change of strain with respect to the blade span.

So far, SPA has only been applied to model rotor blades, but it is hoped to develop the technique to its full potential and to extend its application to wind tunnel and full-scale flight tests. In addition to verifying the predicted mode shapes, the aim will be to derive instantaneous displacements or rotations of the blade at any azimuth station throughout a complete cycle of rotation.

Table 1

Proportions of calibration modes contained within the derived displacement shape of Example 1 (second overtone flap mode)

Calibration mode	Calibration mode proportion			
	A	B	C	D
Fundamental flap	-0.219	-0.336	-0.115	-0.076
First overtone flap	0.076	0.089	0.052	0.055
Second overtone flap	0.969	0.961	0.976	0.970
Third overtone flap	0.027	0.024	0.028	0.026
Fundamental lag	-0.030	-0.010	-0.007	-0.007
First overtone lag	0.034	0.036	0.035	0.035
Second overtone lag	0.002	0.003	0.003	0.003
Fundamental torsion	0.181	0.187	0.182	0.189
First overtone torsion	0.002	0.004	0.001	0.003
Second overtone torsion	0.012	0.012	0.010	0.012
Third overtone torsion	-0.004	-0.004	-0.012	-0.010

Table 2

Proportions of calibration modes contained within the derived displacement shape of Example 2 (third overtone flap mode)

Calibration mode	Calibration mode proportion			
	A	B	C	D
Fundamental flap	1.025	1.188	0.350	0.318
First overtone flap	-0.163	-0.202	-0.079	-0.084
Second overtone flap	0.096	0.114	0.073	0.081
Third overtone flap	-0.957	-0.933	-0.960	-0.944
Fundamental lag	-0.006	0.034	0.010	0.012
First overtone lag	-0.007	-0.006	-0.002	-0.003
Second overtone lag	-0.008	-0.008	-0.011	-0.011
Fundamental torsion	0.136	0.142	0.132	0.130
First overtone torsion	0.192	0.196	0.204	0.203
Second overtone torsion	0.114	0.112	0.120	0.111
Third overtone torsion	0.044	0.051	0.084	0.083

REFERENCES

No.	Author	Title, etc
1	D.R. Gaukroger C.J.W. Hassal	Measurement of vibratory displacements of a rotating blade. Vertica, Vol.2, pp 111-120 (1978)
2	D.R. Gaukroger D.B. Payen A.R. Walker	Application of strain gauge pattern analysis. Paper No.19, 6th European Rotorcraft and Powered Lift Forum (1980)
3	C.J.W. Hassal	Development and initial application of a technique to measure vibration mode shapes of a rotating blade. RAE Technical Report 77064 (1977)
4	A.R. Walker	Application of strain pattern analysis to the derivation of vibration mode shapes of a rotating model helicopter blade. RAE Technical Report 82024 (1982)
5	G.A. Taylor D.R. Gaukroger C.W. Skingle	MAMA - A semi-automatic technique for exciting the principal modes of vibrating complex structures. ARC R&M No.3590 (1967)
6	S.P. King	Blade equations by Hamilton's method using an ordering scheme. WHL Report No. GEN/DYN/209N (1980)
7	A.R. Walker	A comparison between theoretically and experimentally derived vibration mode shapes of a rotating model helicopter blade. RAE Technical Report 82056 (1982)
8	A.R. Walker	A note on strain gauge distribution in the application of strain pattern analysis to helicopter rotor blades. Unpublished MOD Paper (1982)

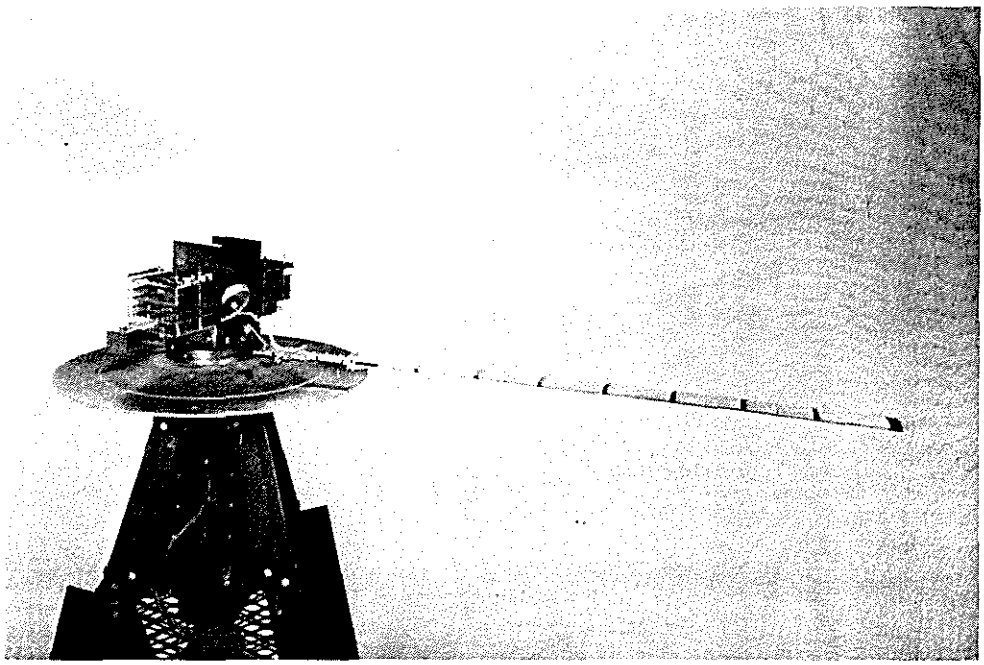

Fig 1 Model blade

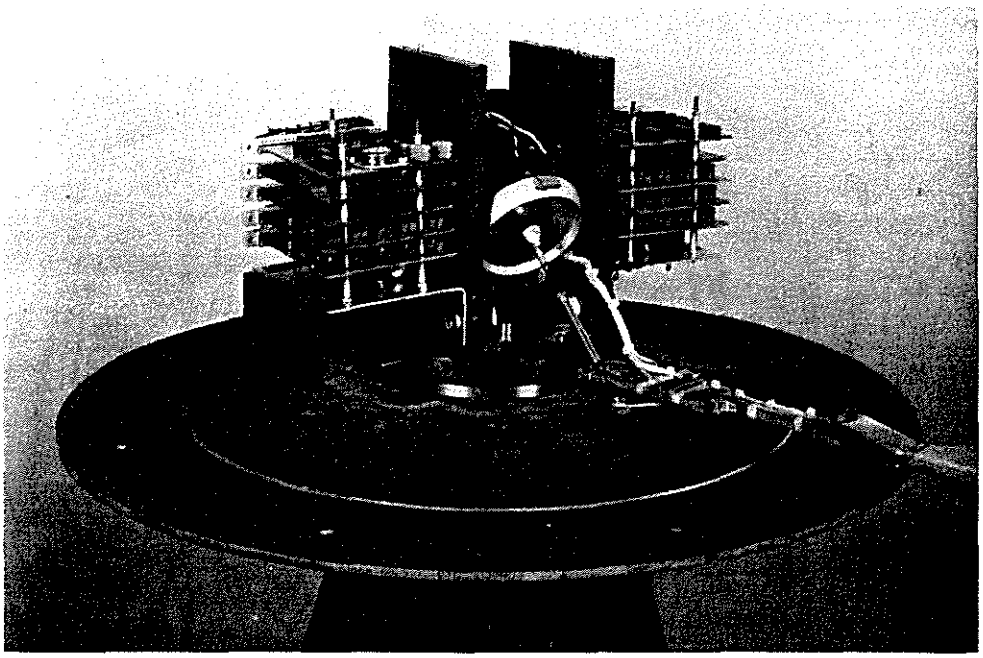

Fig 2 Hub and excitation system

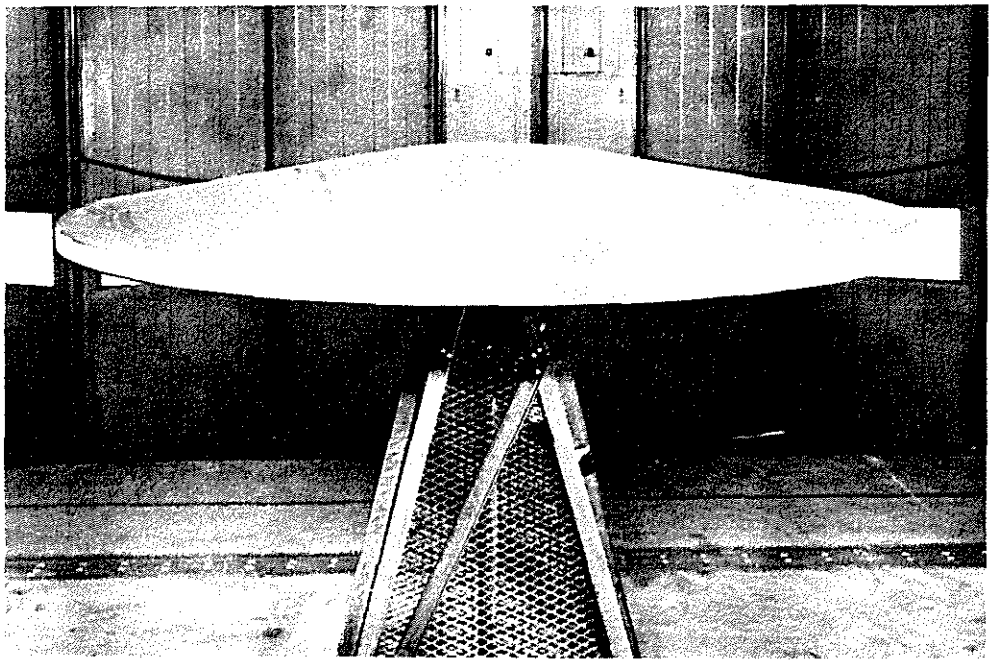

Fig 3 Shielding disc

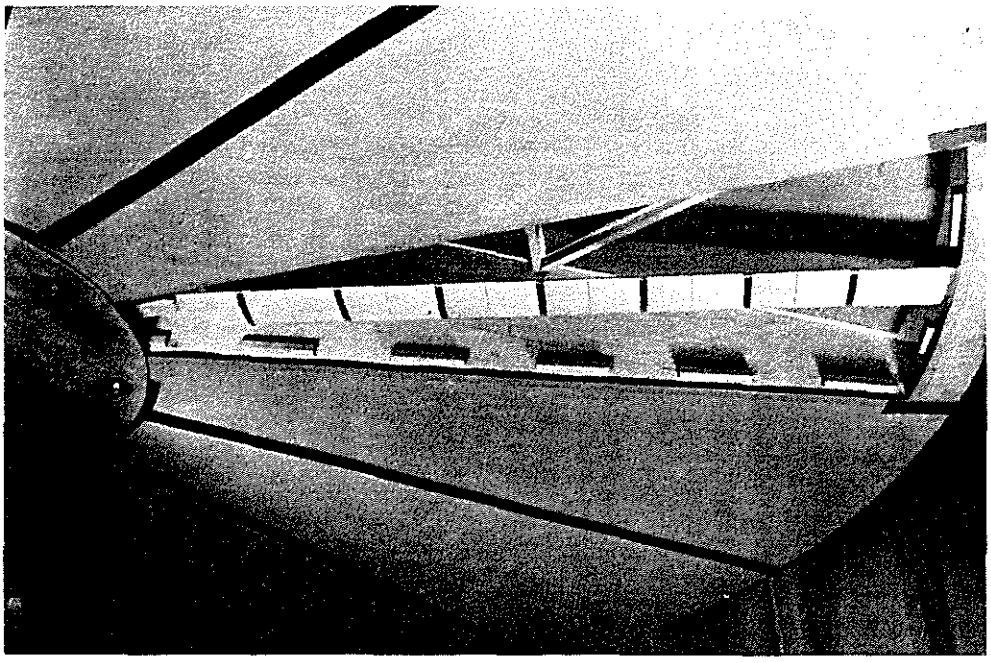

Fig 4 Blade enclosed in shielding disc

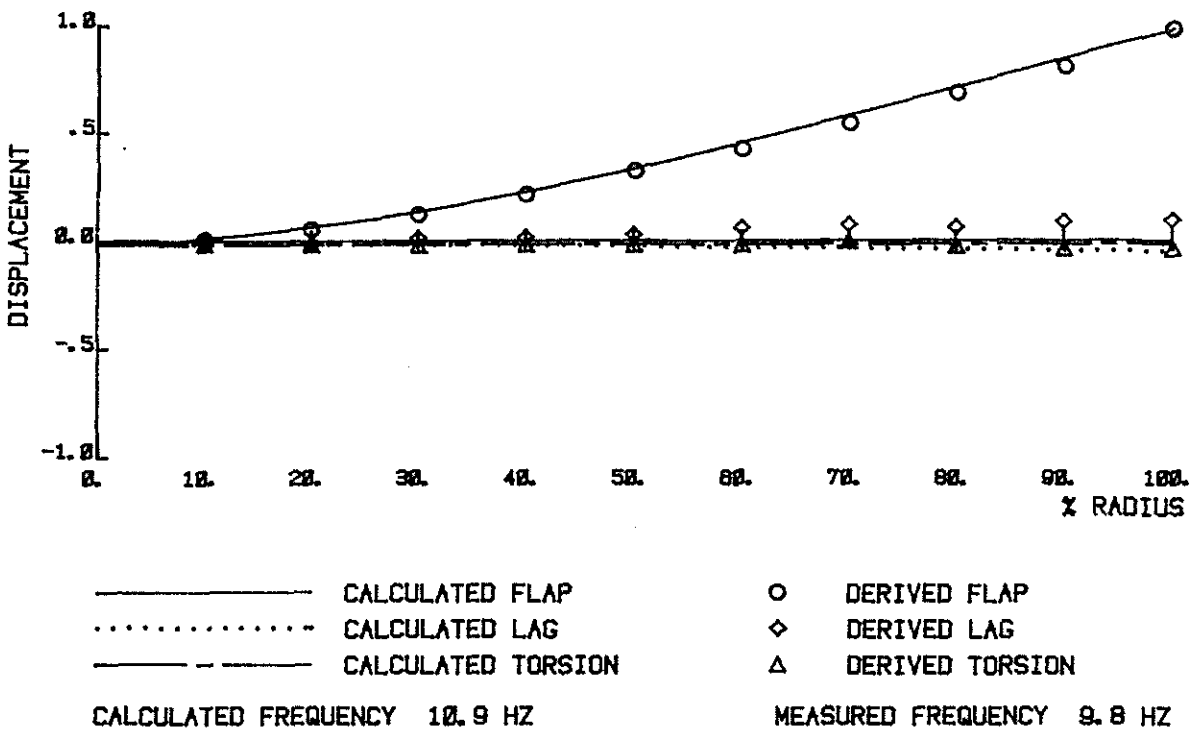

Fig 5 Test Mode 1 Rotor speed 8 rev/s

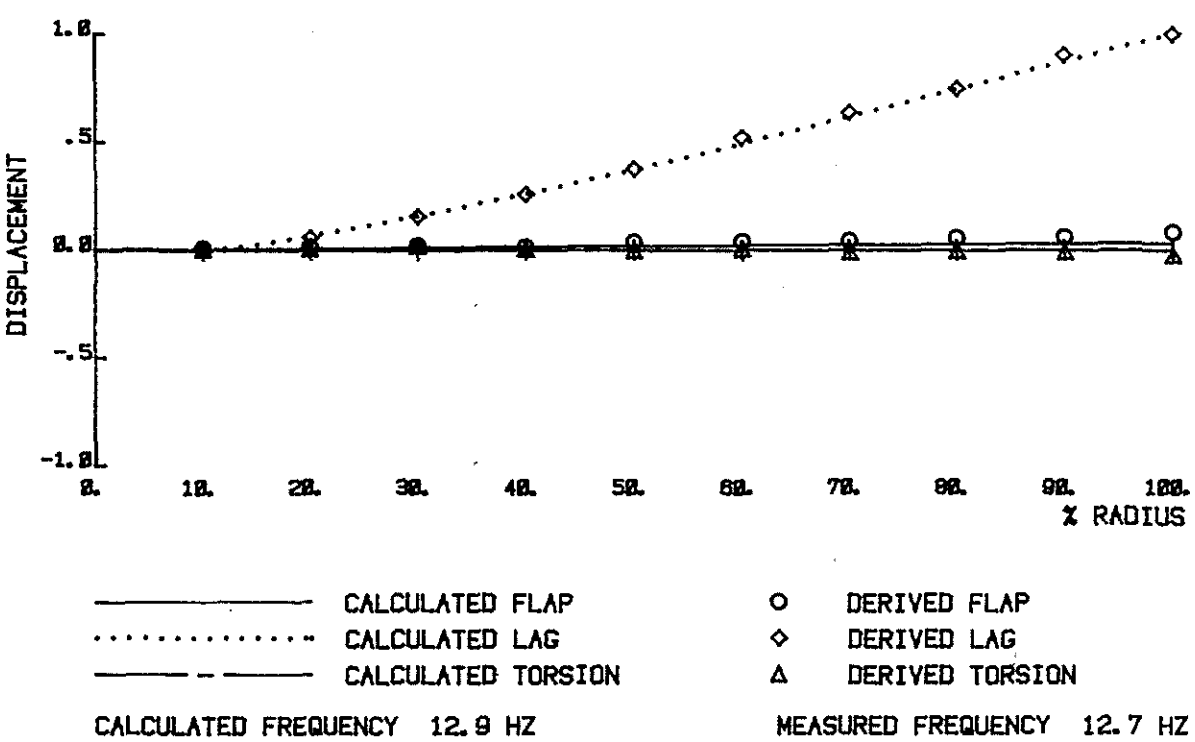

Fig 6 Test Mode 2 Rotor speed 8 rev/s

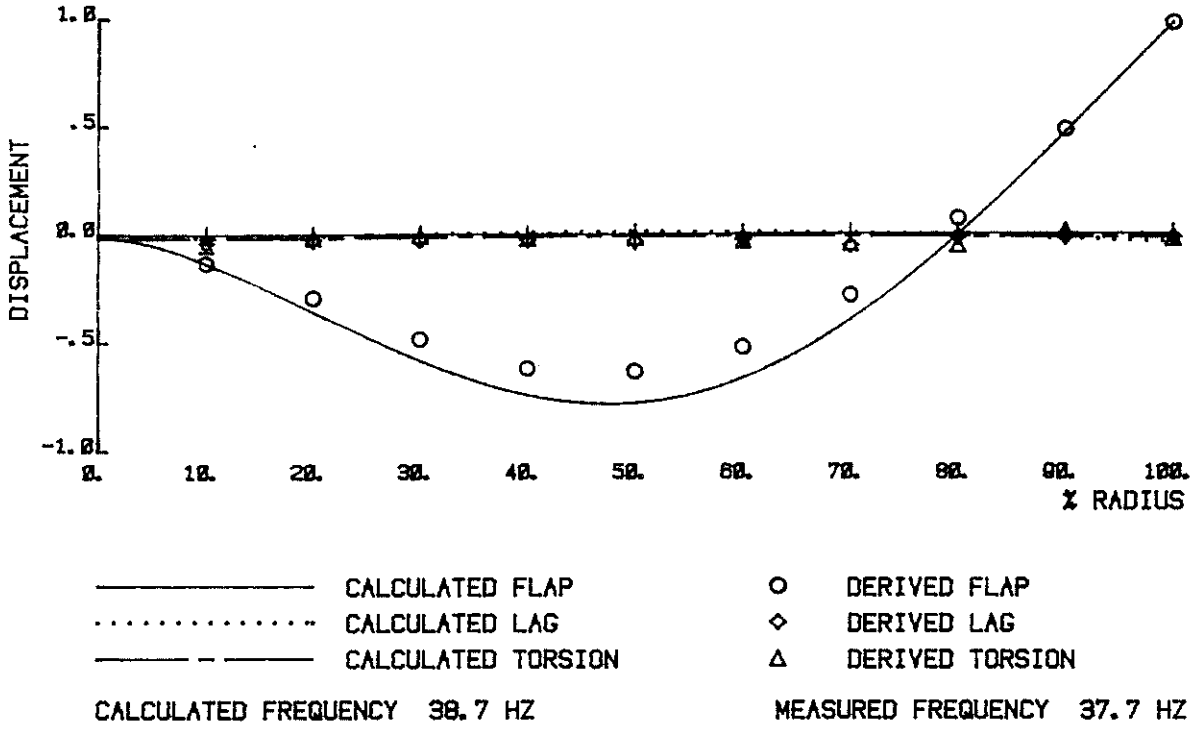

Fig 7 Test Mode 3 Rotor speed 8 rev/s

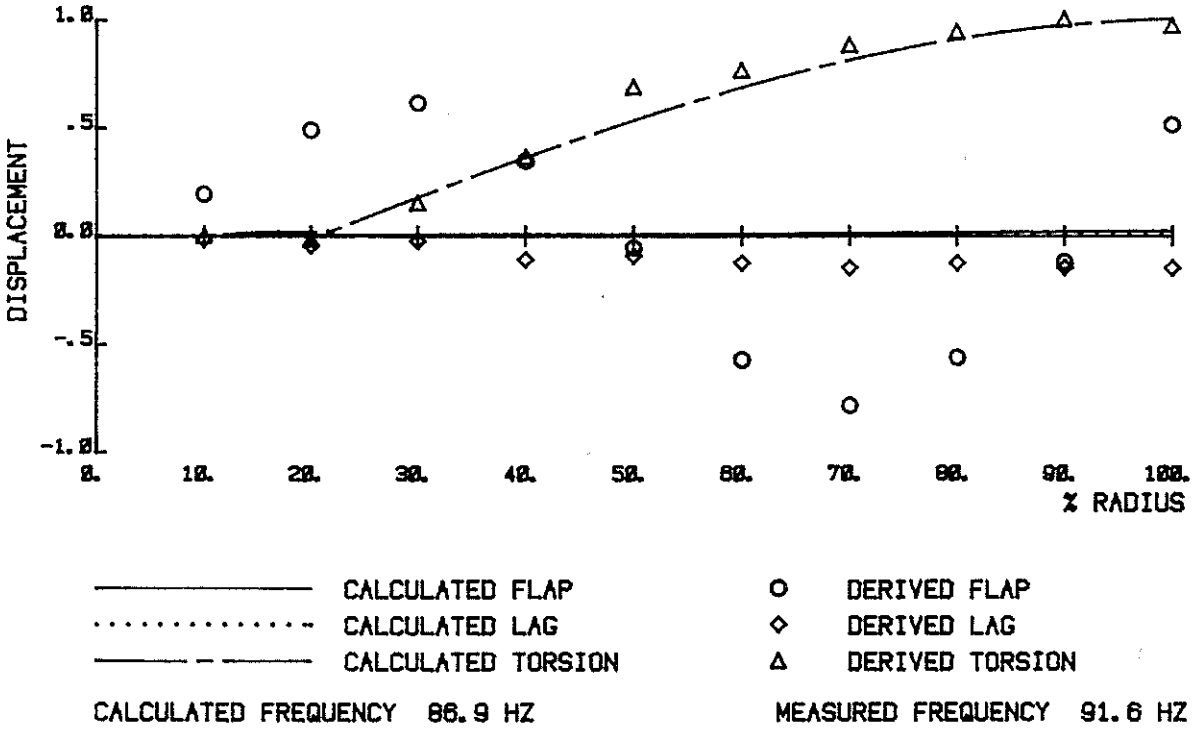

Fig 8 Test Mode 4 Rotor speed 8 rev/s

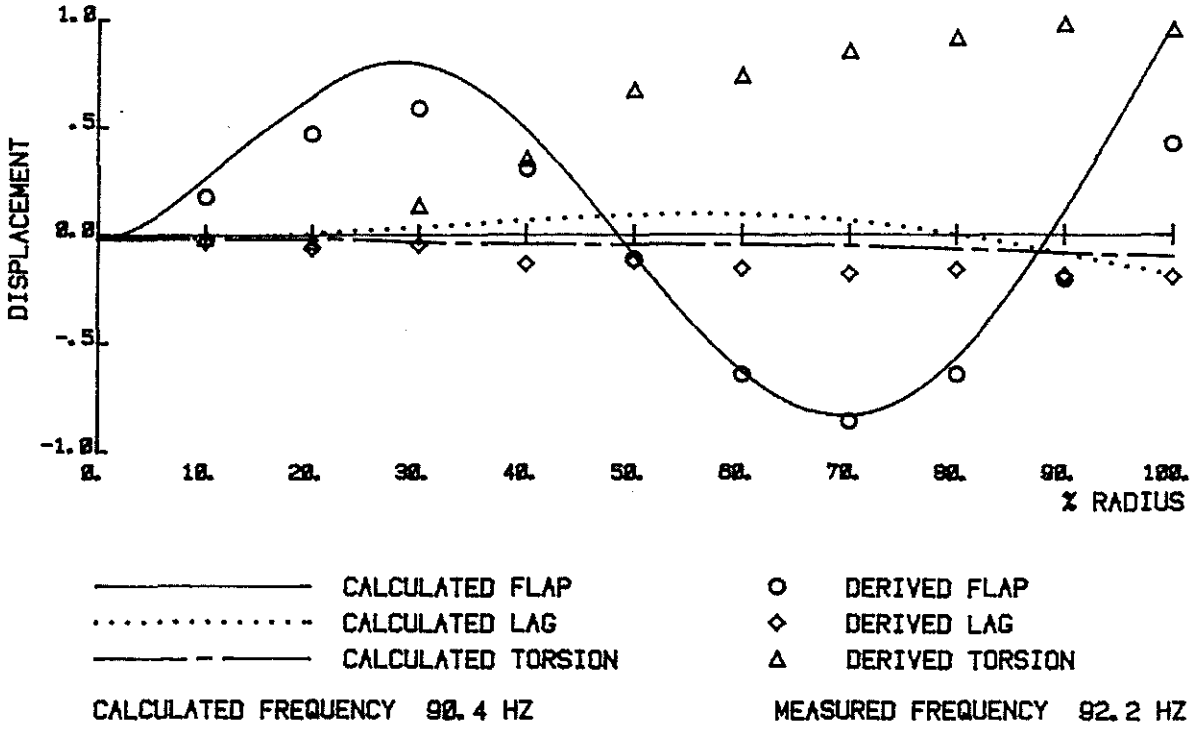

Fig 9 Test Mode 5 Rotor speed 8 rev/s

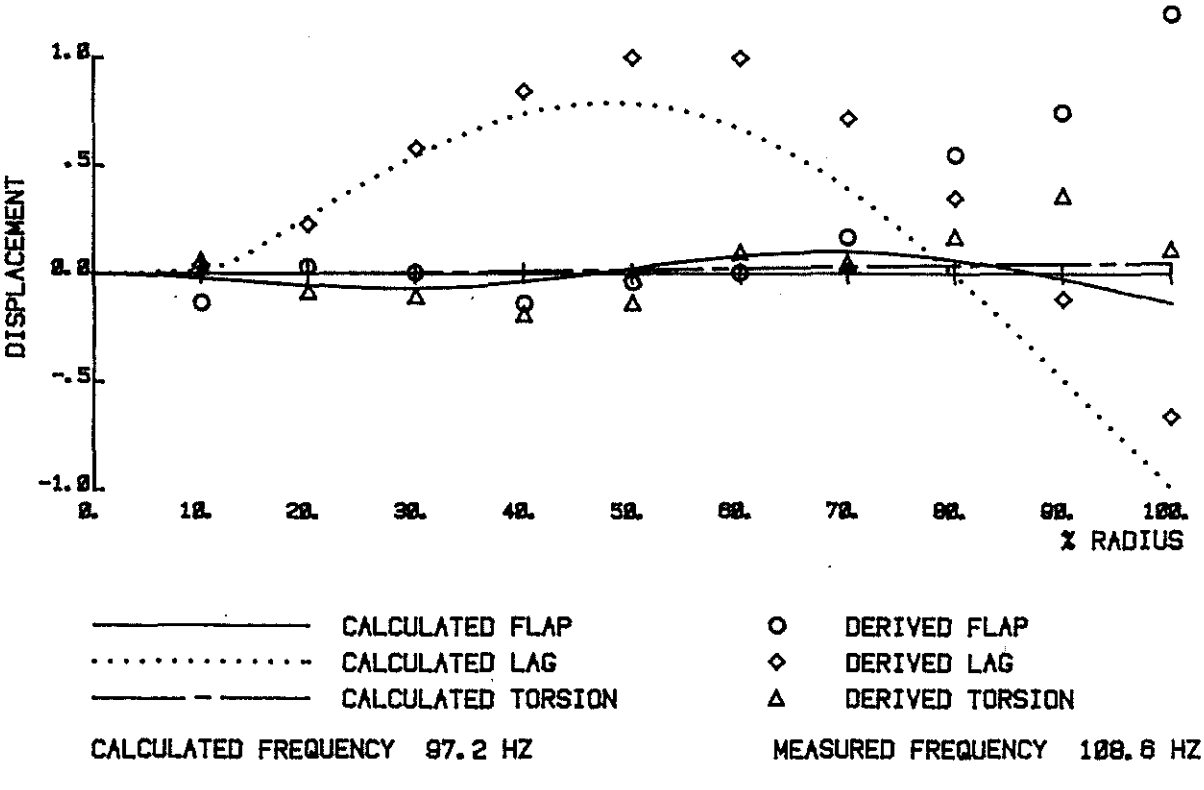

Fig 10 Test Mode 6 Rotor speed 8 rev/s

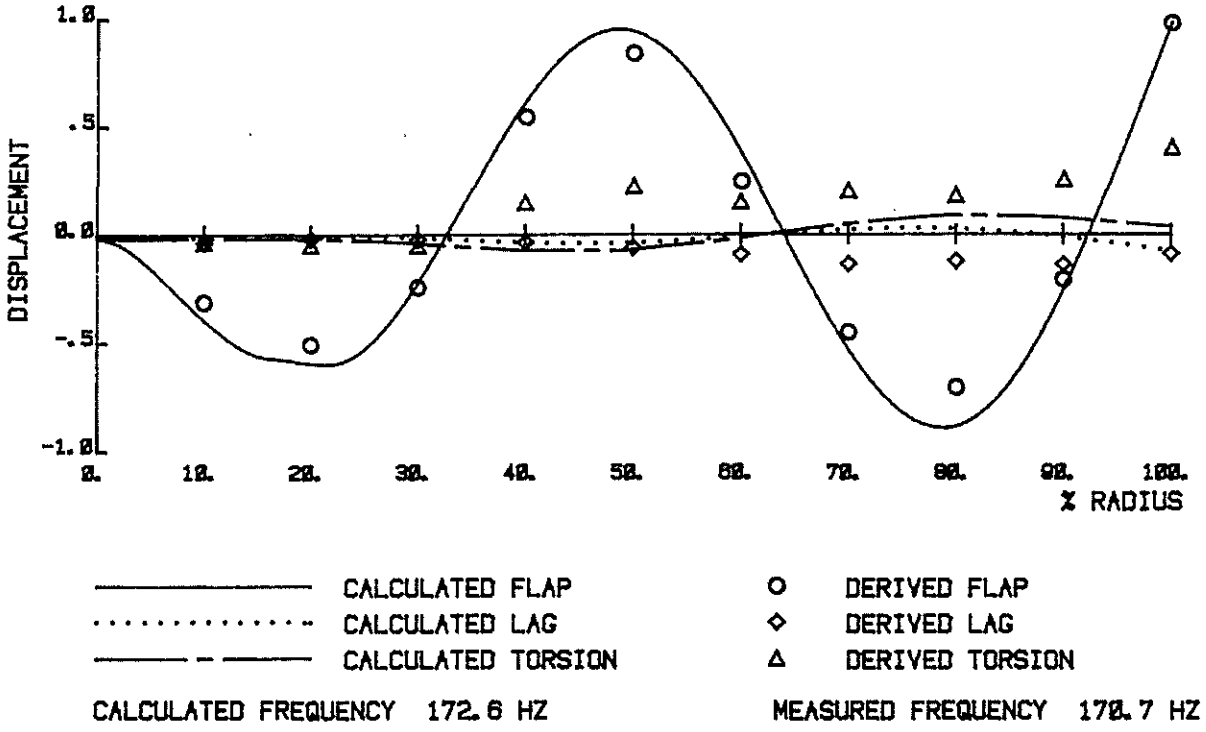

Fig 11 Test Mode 7 Rotor speed 8 rev/s

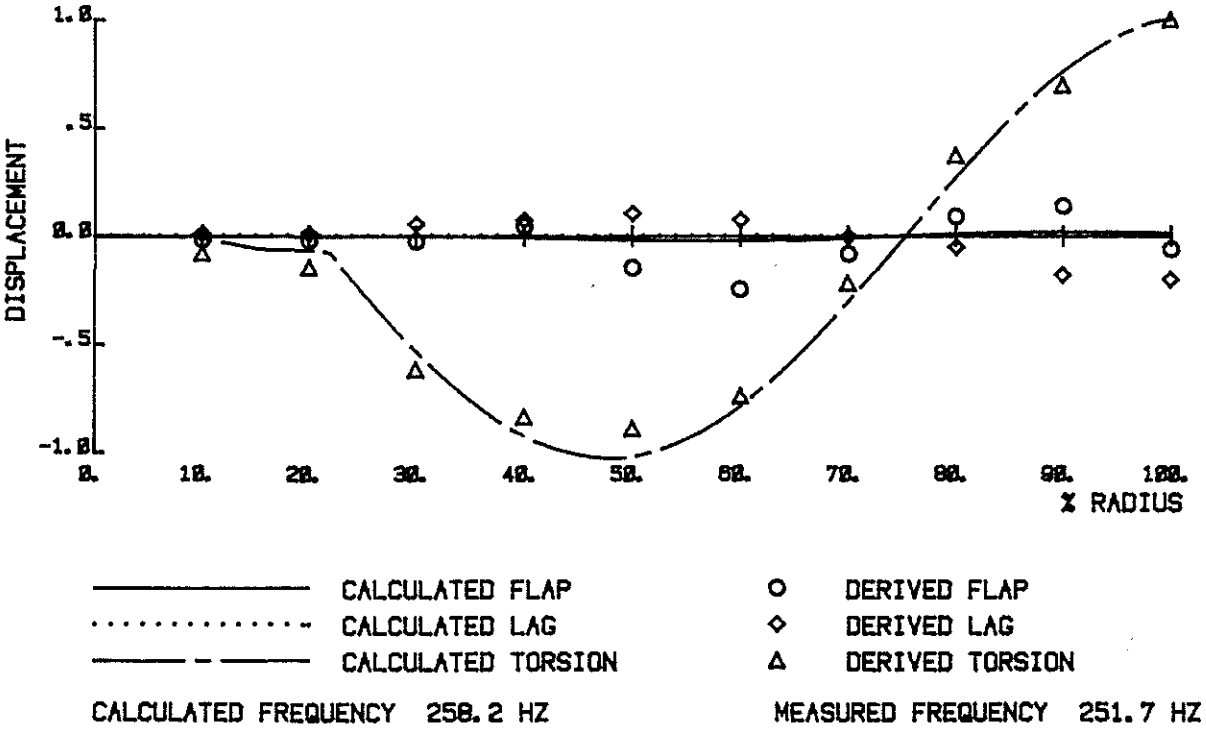

Fig 12 Test Mode 8 Rotor speed 8 rev/s

(a) Blade Profile

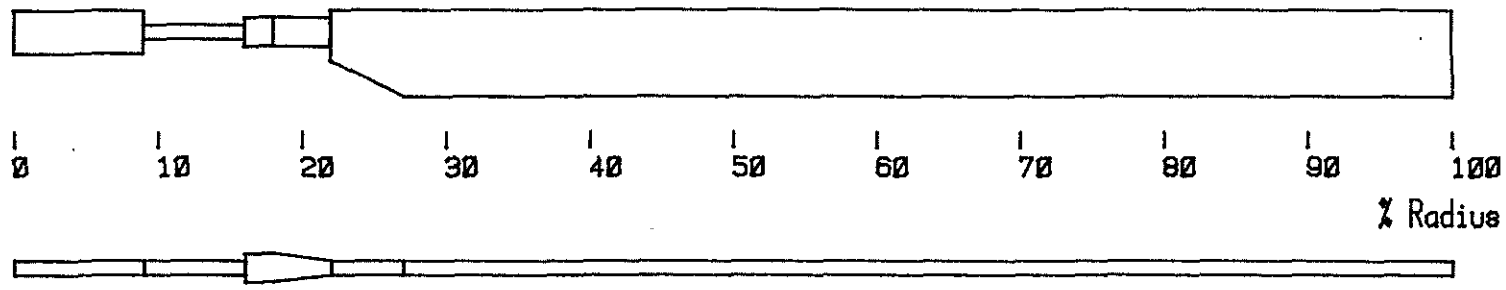

(b) Strain Measurement Stations

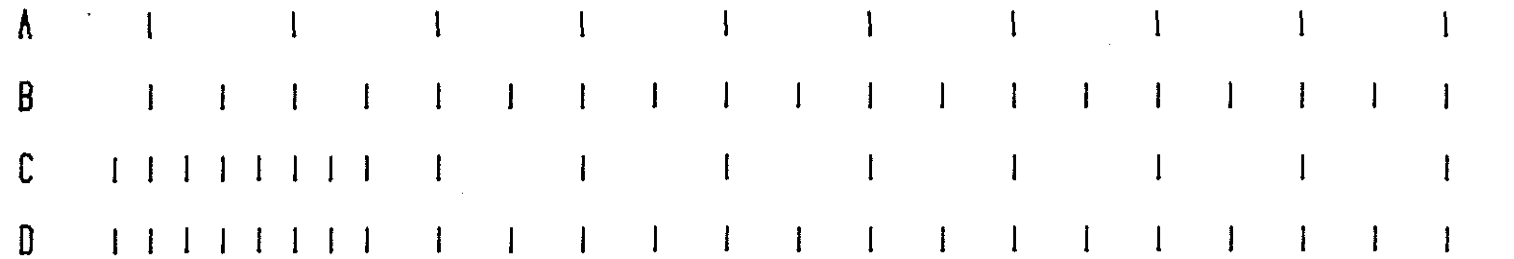

(c) Displacement Measurement Stations

Fig 13 Distribution of strain and displacement measurement stations

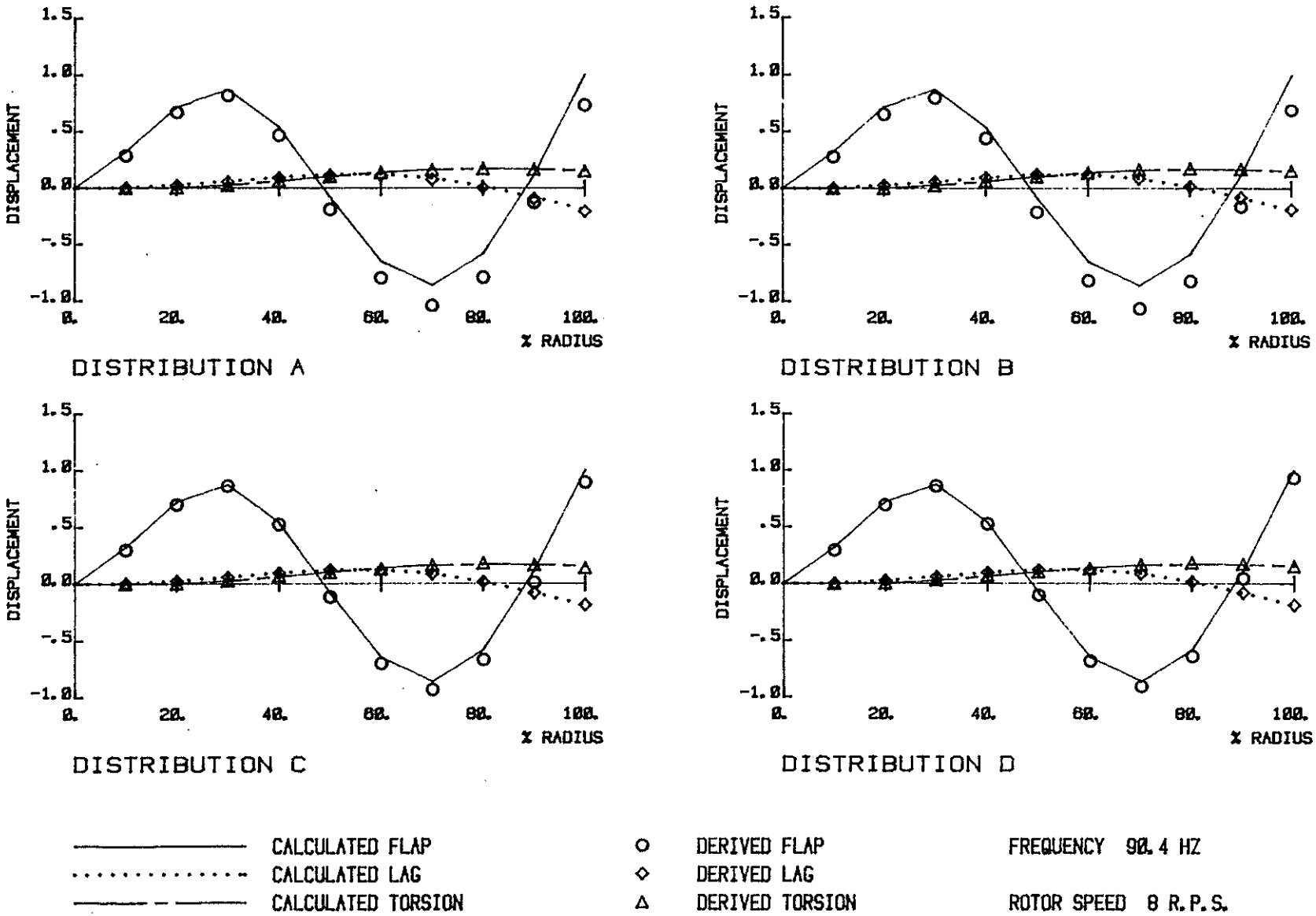

Fig 14 Displacements of Mode 5

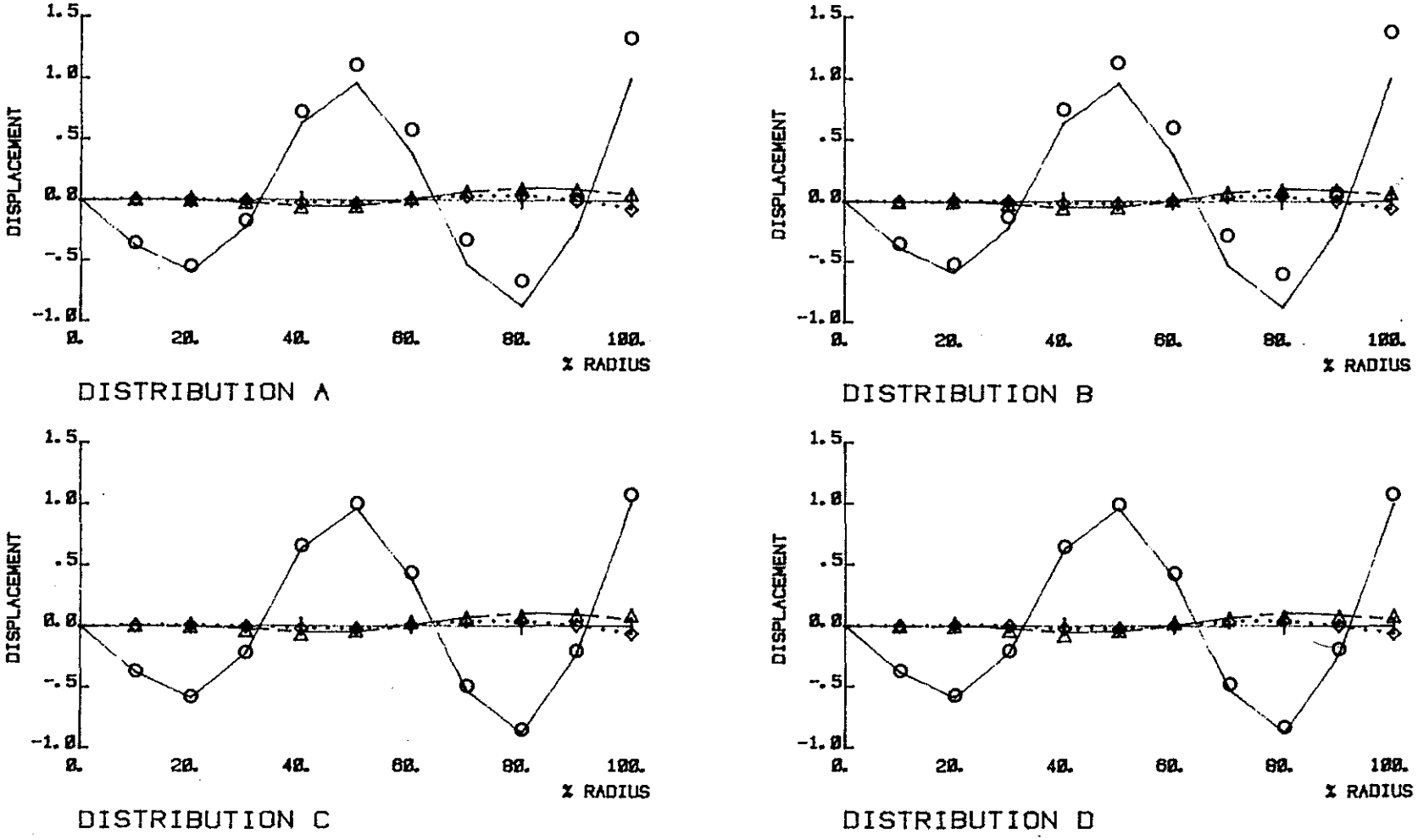

Fig 16 Displacements of Mode 7

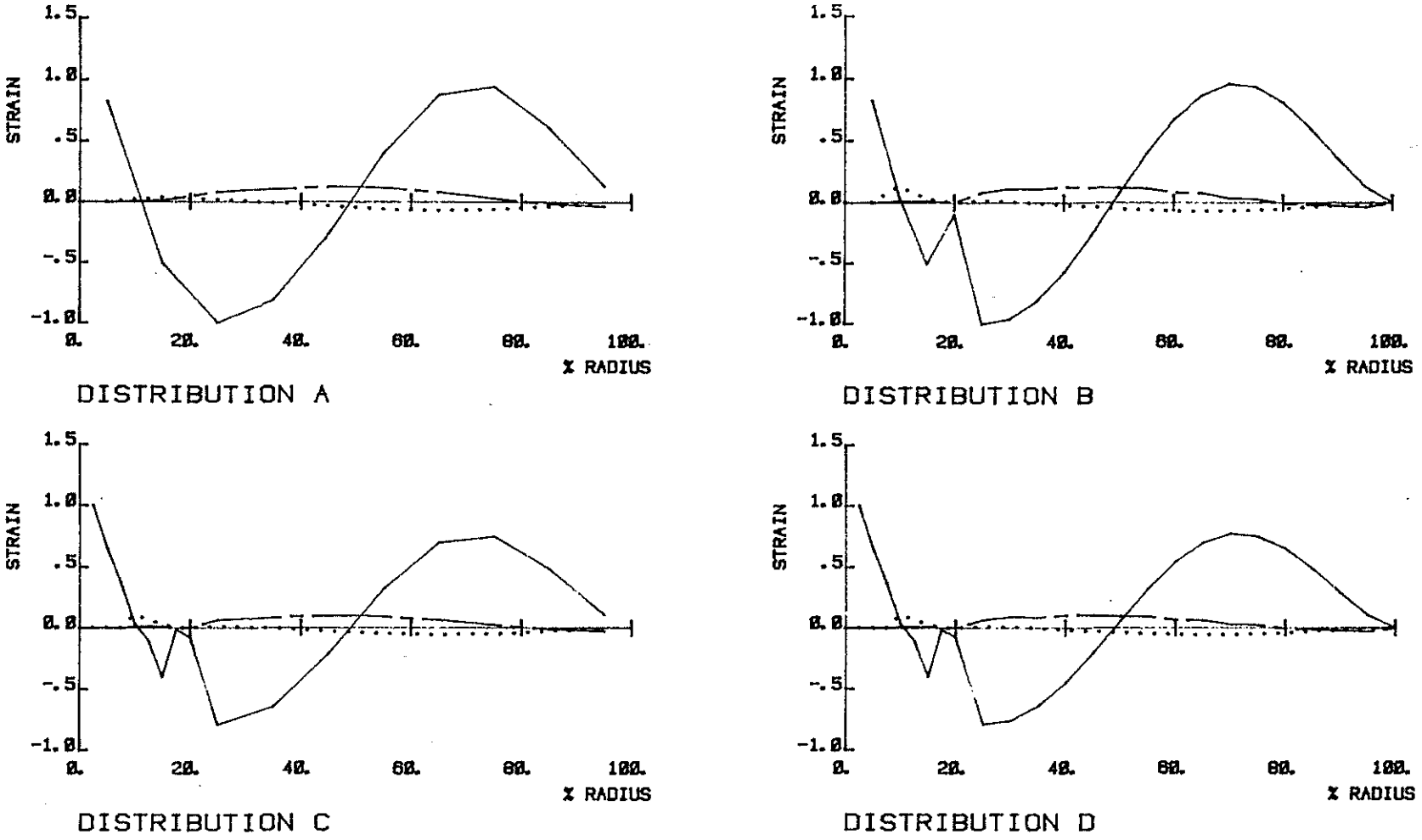

Fig 15 Strain patterns of Mode 5